Journal of Systems Engineering and Electronics
Vol. PP, No. 99, June 2022, pp.1 – 12

EXCLUSIVELY AVAILABLE VIA
IEEE Xplore® DIGITAL LIBRARY

Recognition of dynamically varying PRI modulation via deep learning and recurrence plot

WANG Pengcheng, LIU Weisong, and LIU Zheng*
College of Electronic Science and Technology, National University of Defense Technology, Changsha 410000, China

Abstract: Recognition of pulse repetition interval (PRI) modulation is a fundamental task in the interpretation of radar's intents. However, the existing PRI modulation recognition methods mainly focus on single-label classification of PRI sequences. The prerequisite for the effectiveness of these methods is that the PRI sequences have been perfectly divided according to different modulation types before identification, while the actual situation is that radar pulses reach the receiver continuously, and there is no completely reliable method to achieve this division in the case of non-cooperative reception. Based on the above actual needs, this paper implements an algorithm based on the recurrence plot technique and the multi-target detection model, which does not need to divide the PRI sequence in advance, and compared with the sliding window method, it can more effectively realize the recognition of the dynamically varying PRI modulation.

Keywords: you look only once (YOLO), pulse repetition interval (PRI) modulation, recurrence plot.

DOI: 10.23919/JSEE.2022.000071

1. Introduction

An electronic support system (ESM) is one of the most important equipment in modern warfare. When multiple radars transmit signals at the same time, the ESM will receive interlaced pulse streams. Then, the ESM will separate these signals [1,2] to determine the source radar and analyze the signals of one radar to dig out as much information about it as possible, including its working rules and functional intentions [3]. However, with the further development of radars, understanding their functional intentions becomes increasingly difficult.

In particular, the recognition of radar pulse repetition interval (PRI) modulation has become a core issue of intercept receiver signal processing, because it provides valuable information about the intentions of the radar [4]. PRI is the first-order difference of the time of arrival which demonstrates the intricate patterns, and is a stable radar signal feature that can be easily measured. It is the stability that makes PRI parameters applied to radar signal sorting [5−7] and radar recognition [8,9] tasks.

Traditional PRI modulation recognition is usually achieved by using a histogram of the pulse interval [10,11]. These methods can only recognize simple PRI modulations and rely heavily on the experience of the operator, which can easily lead to missed detections and false detections. With the development of machine learning in recent years, some intelligent methods have been proposed. These methods can be roughly divided into two categories: one is based on artificially designed features [12,13] and classifiers such as multilayer perceptron and support vector machines [14−16] are used to generate classification results. The recognition effect of these methods using artificial features will be greatly reduced under the condition of poor pulse reception, and the reason is obvious: features will lose their regularity under poor pulse reception. The others use neural network methods to automatically extract features and perform classification. For example, Li et al. [17] proposed a one-dimensional PRI modulation recognition method based on convolutional neural network (CNN); in paper [18], long-short term memory (LSTM) network was added after CNN to analyze the temporal structure of the PRI sequence, which achieved better recognition effect. In addition, scholars have also explored the use of full CNN to recognize variable length PRI sequences [19]. Compared with the first two methods, this method has more practical value. With the deep development of machine learning theory, more techniques are used for PRI modulation recognition. Among them, Li et al. [20] proposed an attention-based cyclic neural network, which further improves the recognition performance; Wei et al. [21] proposed to transform

Manuscript received March 12, 2021.
*Corresponding author.
This work was supported by the National Defense Science and Technology Outstanding Youth Science Fund Project (2018-JCJQ-ZQ-023), and the Hunan Provincial Natural Science Foundation of Innovation Research Group Project (2019JJ10004).

the PRI sequence into image, and then used more mature image classification network for recognition. These researchers have achieved good recognition results in the PRI sequences with a single modulation type. However, the prerequisite for the effectiveness of these methods is that the PRI sequences have been perfectly divided according to different modulation types before identification, while the actual situation is that radar pulses reach the receiver continuously, and there is no completely reliable method to achieve this division in the case of non-cooperative reception.

Some researchers have tried to overcome the shortcomings of existing methods. Kauppi et al. [4] proposed a sliding window technique. It stated that the sliding window technique faced the problem of confusion: in the case of a short window, the shape of dwell and switch (DAS) PRI and constant PRI were the same, and the model could not distinguish between these two modulations at all. Confusion can also occur between sine PRI and sliding PRI and between jitter PRI and stagger PRI. The principle is similar. To solve this confusion problem, the author first divided the six modulations into three parent modulations: constant and DAS PRI were subcategories of stable PRI, periodic and sliding PRI were subcategories of directional PRI, and jitter and stagger PRI were subcategories of non-directional PRI. The author further distinguished the sub-modulation from the parent modulation, so as to achieve a hierarchical recognition. Although this method successfully solves the problem of identification and boundary detection of the parent modulation, when the sequences of the two sub-modulations are connected, this method cannot further divide them, which is a major flaw of the method, and the recognition efficiency is not high due to the use of the sliding window technique. In conclusion, the sliding window technique has limitations and is an incomplete solution to the drawbacks of the existing methods.

This article improves the current situation by proposing a method based on the recurrence plot and you look ony once (YOLO) algorithm which is called RP-YOLO, it can be applied to reveal dynamically varying PRI modulations. To our best knowledge, this is the first time that the recurrence plot is used to represent different PRI sequences in radar field. The core idea of this article is to regard the recognition and location of multiple modulations in the PRI sequence as a multi-target detection problem. In particular, this article considers turning the PRI sequence into a suitable two-dimensional image form and uses the YOLO algorithm to achieve efficient detection. Experimental results show that the proposed RP-YOLO method is effective and robust even under contaminated data.

The remainder of the paper is organized as follows. The basic six PRI modulation types are presented in Section 2. In Section 3, the proposed RP-YOLO method is discussed in detail. In Section 4, the effectiveness and robustness of the proposed method are demonstrated through simulation. Finally, conclusions are drawn in Section 5.

2. PRI modulations

The PRI modulation can be expressed by the following formula [4]:

$$t_{k+1} - t_k = x_k,\ \ k = 0, 1, \cdots, N-1 \tag{1}$$

where t_k is the pulse arrival time, x_k represents the pulse time interval, N denotes the total number of pulses. In general, PRI modulation can be divided into six types: constant, jitter, DAS, sliding, sine, and stagger, which means that K has six variables. Examples of the six modulations are shown in Fig. 1 and Fig. 2, and a brief description of these PRI modulations is given below.

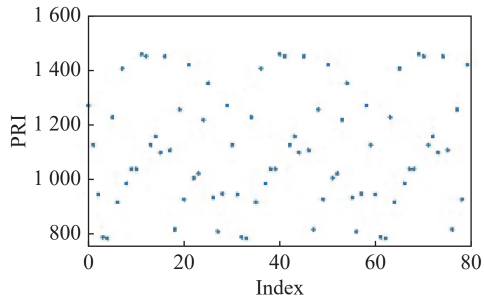

(a) Stagger

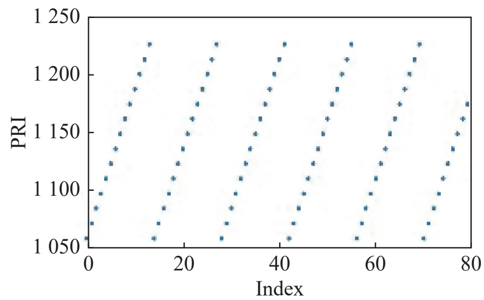

(b) Siding

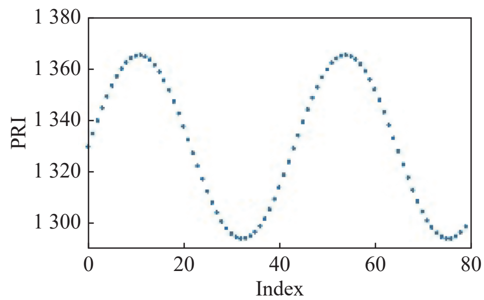

(c) Sine

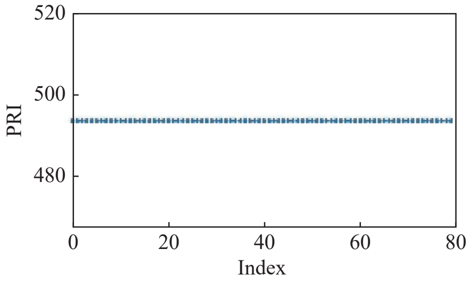

(d) Constant

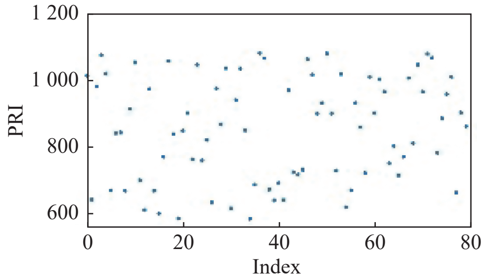

(e) Jitter

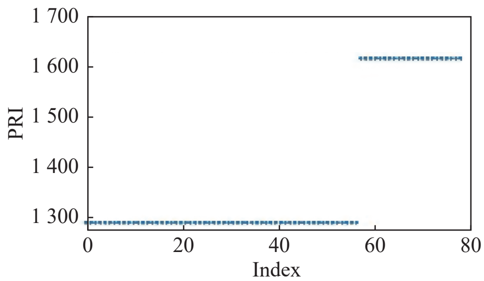

(f) DAS

Fig. 1 Six types of PRI modulations in ideal environment

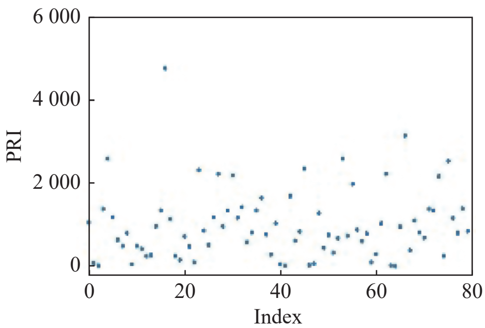

(a) Stagger

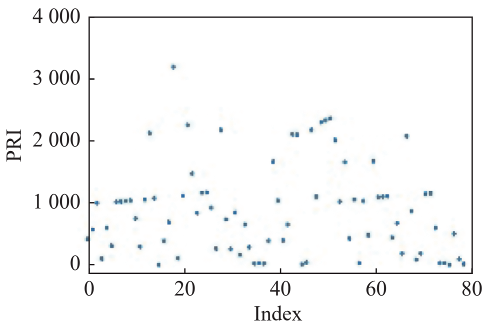

(b) Sliding

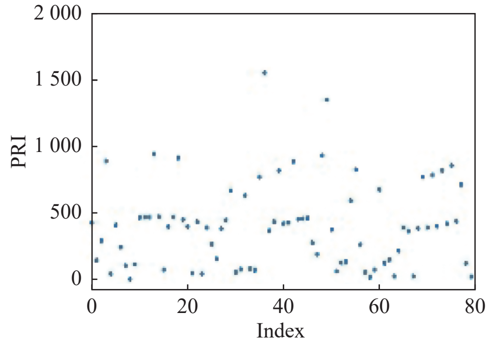

(c) Sine

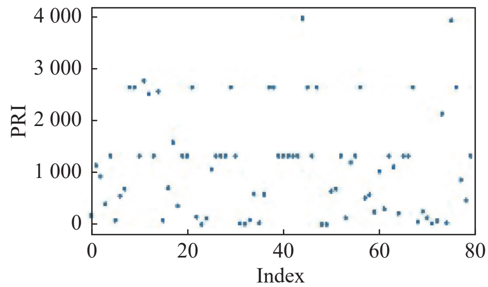

(d) Constant

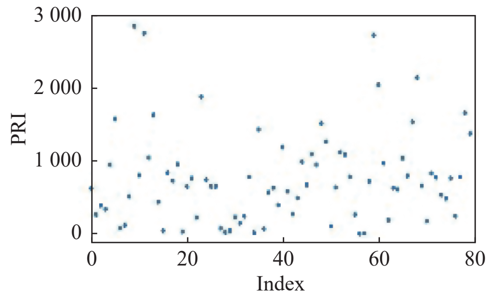

(e) Jitter

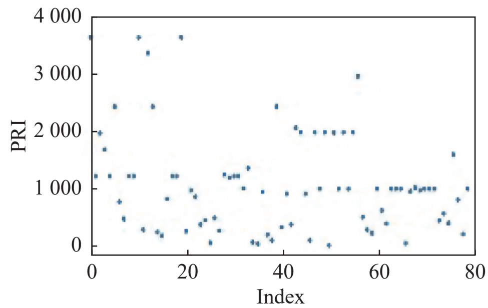

(f) DAS

Fig. 2 Six types of PRI modulations in real electronic warfare environment

Constant PRI: The constant PRI sequence has a stable value and the variation is less than 1% of the average PRI value. This modulation is often used for searching and tracking tasks.

Stagger PRI: For stagger PRI sequences, several (usually 2 to 7) stable PRI values appear in cyclic order or randomly. This modulation is often used to eliminate blind speed in moving target indication.

DAS PRI: The difference between DAS PRI and stagger PRI is that DAS PRI's value is maintained at a specific value for a period of time, and then switched to another for a period of time. These maintained PRI values may repeat regularly or irregularly. This modulation is used to solve speed or distance ambiguity problems.

Jitter PRI: The value of jitter PRI is jittered around a certain PRI value and is a random variable that follows a Gaussian or uniform distribution. The jitter range is between 1% and 30% of the average PRI value. This modulation is often used to fight forward interference.

Sliding PRI: The pulse interval in the sliding PRI sequence increases or decreases linearly. Sliding is usually periodic, and when one limit is reached, it will quickly switch to another limit. This modulation is commonly used to provide high coverage in pitch scans.

Sine PRI: The sine PRI sequence is expected to have a small change of less than 5% in the average pulse repetition rate at a frequency of about 50 Hz. This modulation is often used for missile guidance.

3. Method

3.1 Preprocessing

Recurrence plot was first proposed by Eckmann et al. [22] in 1987, which is mainly used for the qualitative analysis of nonlinear dynamic systems and can realize a graphical representation of system states. It has been successfully applied in many fields such as climate change [23], earth science [24], and engineering [25]. In the radar field, the switching of the modulation in the PRI sequence reflects the dynamic changes of working intention inside the radar. This article treats the PRI sequence as the observation data of a complex system like radar and uses the recurrence plot, a method of studying complex systems, to study radar.

This article first continuously intercepts sequences of length N from a long sequence, and calculates the distance between any two points in the sequence to obtain an $N \times N$ distance matrix $\boldsymbol{R}_{i,j}$.

$$\boldsymbol{R}_{i,j} = \mathrm{dist}(x_i, x_j), \quad 0 \leqslant i, j \leqslant N \tag{2}$$

where $\mathrm{dist}(\cdot)$represents the Euclidean distance. Next, this article scales the distance matrix's value range and turns it into a grayscale image as the final sequence representation result. In the grayscale image, if two points in the sequence are close enough, the distance between them will be close to 0 and the corresponding pixel in the image is a black point, otherwise, the pixel at the corresponding position is a white point. The graphical representation of $\boldsymbol{R}_{i,j}$ is called recurrence plot.

Recurrence plot can effectively represent the characteristics of PRI modulations. Fig. 3 shows six recurrence plots under the ideal reception conditions (Fig. 3) and real electronic warfare environment (Fig. 4). Under the ideal reception condition, the constant PRI sequence has only one value, and the distance between all points is 0, so its recurrence plot is all black pixels. The recurrence plot of the ideal DAS PRI sequence looks like a chessboard, which represents the sudden switching of values and periodic cycles and that the value within one period remains stable. Because the values in the jitter PRI sequence vary randomly, its recurrence plot shows a random distribution of black and white pixels as a whole. The values in the ideal sine PRI sequence are continuous and cyclically changing, so the white pixels and black pixels are dotted and distributed across.The ideal sliding PRI is also a periodic sequence, so its recurrence plot has the shape of a small square, and since in each cycle, the sliding PRI changes linearly, each row of its recurrence plot presents a gradual characteristic. The stagger PRI is a group of several fixed PRI values and appears periodically, its recurrence plot appears periodically in small squares, and the number of small squares in each row and the number of repetition periods of the sequence are the same. In the case of highly non-ideal reception (Fig. 4), the characteristics of these PRI modulations are partially retained in the recurrence plots.

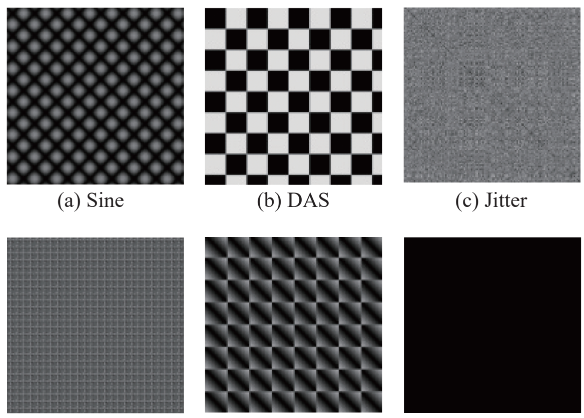

(a) Sine (b) DAS (c) Jitter

(d) Stagger (e) Sliding (f) Constant

Fig. 3 Recurrence plots of six modulations in ideal environment

Further, this article connects the six ideal PRI modulation sequences end to end to form a long sequence, and then uses the recurrence plot method to process the long sequence and obtain the result shown in Fig. 5. It can be seen from Fig. 5 that different PRI modulations produce different structures in the recurrence plot and the structures are distributed in independent squares on the diagonal. The position information of different modulations in the long sequence is included in the pixel coordinates of the recurrence plot. For example, the jitter PRI sequence appears first and its length is 300, then its corresponding substructure will appear in the first square on the diagonal of the recurrence plot. Its coordinates of the upper left corner of this square are (0,0), and its coordinates of the lower right corner point are (300,300). The stagger PRI sequence follows the jitter PRI sequence, and its length is 200. Then the corresponding substructure it generates will appear in the second square on the diagonal of the recurrence plot. The coordinates of the upper left corner of this square are (301,301), and the coordinates of the lower right corner point will be (501,501). Position information of substructures generated by other PRI subsequences can be calculated in the same way.

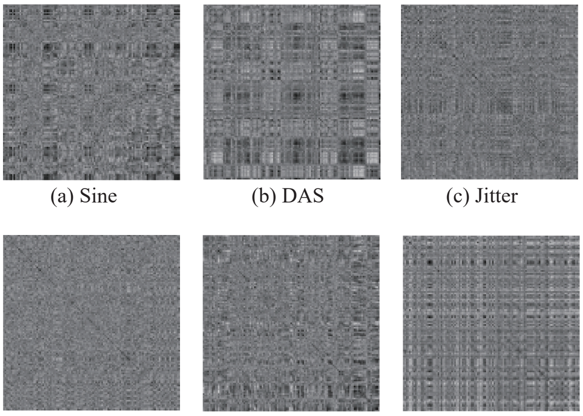

Fig. 4 Recurrence plots of six modulations in real EW environment

3.2 Multi-modulation detection

Since the PRI sequence is preprocessed into the form of a recurrence plot, if the substructures corresponding to different modulations can be automatically identified and located from the recurrence plot, the task of identifying the dynamically varying PRI modulations is completed. This is a multi-target detection problem, and YOLO is one of the most excellent algorithms in the field of image multi-target detection [26−29]. Its core idea is to regard the target detection task as a regression problem of target region prediction and category prediction. Specifically, the YOLO algorithm uses a single neural network to directly predict item boundaries and category probabilities to achieve end-to-end item detection, which is very fast and accurate, its related variants are widely used in various scenarios [30−32].

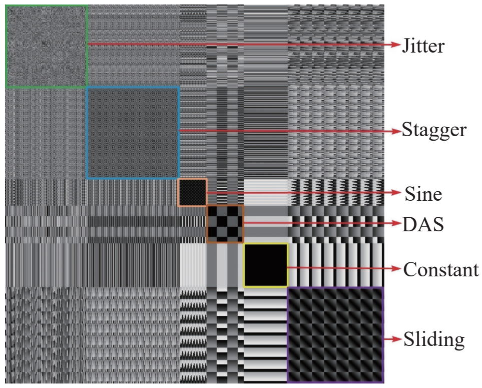

Fig. 5 Recurrence plot corresponding to the end-to-end connection of six PRI sequences

Given these advantages, this article uses the YOLO version 4 (YOLOv4) [29] algorithm to detect the substructures corresponding to multiple modulations in the recurrence plot, and the network structure of YOLOv4 is shown in Fig. 6.

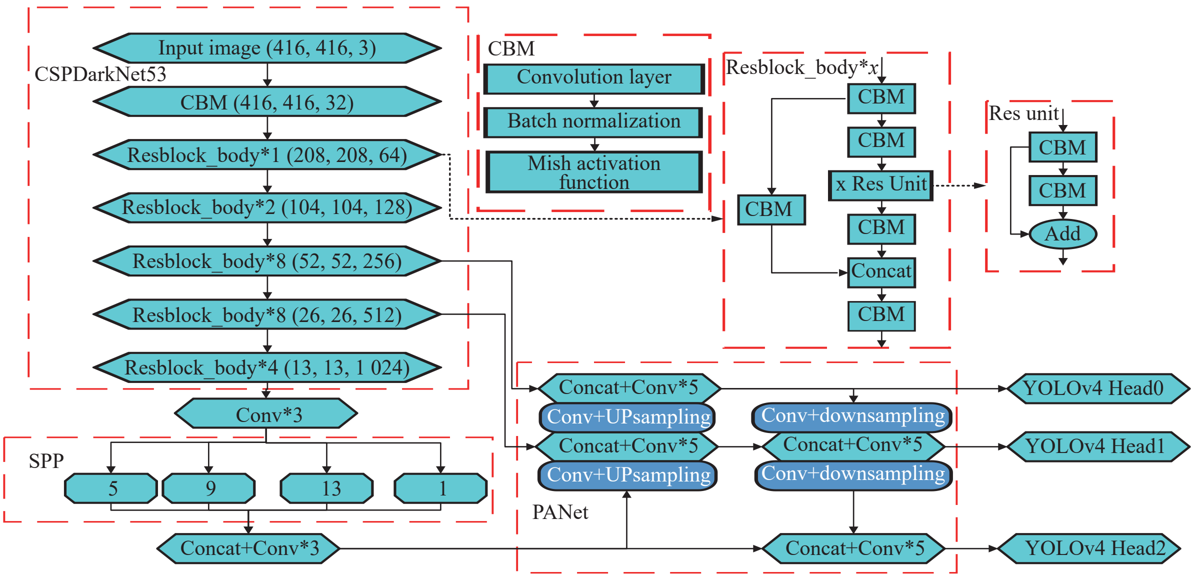

Fig. 6 YOLOv4 network structure

The YOLOv4 algorithm is based on the YOLOv3 algorithm, and introduces optimization methods in data preprocessing, feature extraction network and activation function, which greatly improves the detection speed and accuracy of the model. The backbone network of YOLOv4 adopts Cross Stage Partial Darknet53(CSPDarknet53) network, which has five CSP modules and is different from the residual structure in Darknet53. The CSP module divides the feature mapping of the basic layer into two parts, and then combines the cross stage structure to reduce the amount of calculation and ensure the accuracy. In order to prevent the loss of pooled information, CSP-Darknet53 network still adopts the full CNN method to extract features by convolution instead of pooling. YOLOv4 only uses the mish activation function in the backbone network, and the rest uses leaky relu activation function.

The spatial pyramid pooling (SPP) layer concatenates the pooled feature maps from different core sizes as output. It is found that it is more effective in increasing the receptive field of the backbone network and separating the most important contextual features than simply using the maximum pool of the single core size.

Deep features contain global semantic information, while shallow features contain local feature information. In order to promote the flow of information and shorten the information path between shallow and deep features, YOLOv4 introduces the path aggregation network (PANet) to repeatedly fuse and extract the three feature layers, and finally generate three feature layers, which are 13×13, 26×26, 52×52 to detect large targets, medium targets and small targets respectively.

4. Experiment

To verify the effectiveness and superiority of the RP-YOLO method, this article conducts sufficient contrast experiments. Synthetic data generation and evaluation metrics are described in Subsection 4.1. Then Subsection 4.2 and Subsection 4.3 respectively discuss the advantages of recurrence plot preprocessing and the effectiveness and rapidity of the proposed RP-YOLO method.

4.1 Experiment description

4.1.1 Synthetic data generation

The PRI sequences of this paper are all generated according to parameters in Table 1. From a statistical point of view, the various PRI modulations overlap numerically. In real world situations, the receiving quality of the PRI sequence is affected by some electromagnetic factors. For example, the noise of the measurement circuit and environmental noise will introduce measurement errors. The improper design of the pulse sorter will introduce spurious pulses. Factors such as the azimuth relationship, the system in which the receiver processes the signals that arrive at the same time, and the errors caused by the signal sorting will cause the pulses obtained by the score to be lost. This article assumes that in actual situations, at most 50% of pulses will be lost, at most 40% of pulses are spurious, and that there would be slight measurement uncertainty during normal system operation.

Table 1 Description of the sequences

Method	Parameter							
	Deviation of the average PRI	Number of bursts	Length of the burst in pulse	Number of periods	PRI	Missing pulse’s rate	Spurious pulse’s rate	Measure noisy standard deviation (us)
Jitter	5%−40%	−	−	−	100−200	0%−50%	0%−40%	0−3
Sliding	1:10	−	−	3−10				
Sine	5%−20%	−	−	3−10				
DAS	−	2−8	20−200	−				
Stagger	−	2−64	−	20−40				

A good method should be robust enough to correctly identify the modulation of the sequence contaminated by non-ideal electromagnetic factors.

To consider the individual influence of these factors on classification effect, this article designs three basic non-ideal situations, namely, measuring noise scene only, missing pulses scene only and spurious pulses scene only. In the case of measuring noise, the mean value of the measured noise is 0, the standard deviation is from 0 μs to 3 μs, and the simulation step length is 0.3 μs. The pulse is randomly lost in the case of missing pulses, and the PRI value of a pulse after the missing pulse becomes its own value plus the PRI value of the missing pulse. The ratio of missing pulses ranges from 0% to 50% with a simulation step size of 5%. In the case of spurious pulses, spurious pulses are randomly inserted between two pulses, and the PRI value corresponding to the inserted pulse is split into two values. The rate of spurious pulses ranges from 0% to 40% with a simulation step size of 4%.

To further study the comprehensive influence of the three electromagnetic factors on classification effect, and to get closer to the real reception situation, this article sets up eleven hybrid non-ideal reception scenes in Table 2. From scene 1 to scene 11, the receiving environment gets worse and worse, and the challenge to the robustness of the models is increasing.

Table 2 Parameters of 11 hybrid scenes

Scene	Measuring noise/ μs	Spurious pulse/ %	Missing pulse/ %
1	0.0	0	0
2	0.3	5	4
3	0.6	10	8
4	0.9	15	12
5	1.2	20	16
6	1.5	25	20
7	1.8	30	24
8	2.1	35	28
9	2.4	40	32
10	2.7	45	36
11	3.0	50	40

4.1.2 Evaluation metrics

Accuracy is a traditional evaluation metric of classification model, which calculates the ratio of correctly classified sequence samples. However, in this paper, different segments of PRI sequences are labeled differently, so the calculation method of accuracy needs to be adjusted. For convenience, the label of the PRI segment is assigned to all the pulses in the segment, and the label of unlabeled segments are set to 0. That is, each pulse gets a label. Then, the recognition accuracies for the sequence with a single modulation type and the sequence with multi-modulation types are calculated as follows.

Sequence with single modulation type:

$$\mathrm{acc}_{\mathrm{ssm}} = \frac{1}{N}\sum_{i=0}^{N} I(\hat{y}_i = y_i) \tag{3}$$

Sequence with multi-modulation types:

$$\mathrm{acc}_{\mathrm{smm}} = \frac{1}{N \times M}\sum_{i=1}^{N}\sum_{j=1}^{M} I\left(\hat{y}_i^j = y_i^j\right) \tag{4}$$

In (3) and (4), N is the number of samples in the test set. $\hat{y}_i$ represents the predicted label of the sequence with a single modulation type, and y_i represents the corresponding true label. $\hat{y}_i^j$ represents the predicted label of the jth pulse of the ith sequence that has multiple modulation types. M is the number of pulses for the ith testing PRI sequence.

4.2 Comparison of feature extraction capabilities

In order to compare the performance between preprocessing the PRI sequence with recurrence plot and directly sending the PRI sequence into deep network, three advanced PRI modulation recognition methods are implemented in this paper.

(i) CNN: A one-dimensional PRI modulation recognition method based on CNN [17].

(ii) CNN-LSTM: A network with LSTM unit added to the back of CNN, which can deal with the timing characteristics of the PRI sequence [18].

(iii) RP-Darknet53: The recurrence plot method is used to preprocess the PRI sequence as the input of Darknet53 network, and a softmax layer is added to the Darknet53 network [28].

This section produces sequences samples that have only one single modulation segment with a corresponding label, and these samples are designed to train the above three models. Further, we set the training dataset to contain only six of the 11 hybrid scenes, which are scene 1, scene 3, scene 5, scene 7, scene 9 and scene 11, and there are 1 000 training samples for each modulation in each scene. The test dataset includes three basic non-ideal situations and 11 hybrid non-ideal situations, and there are 500 testing samples for each modulation in each scene.

Fig. 7 shows the comparison results of the recognition accuracy. Generally speaking, these three models are not sensitive to three independent non-ideal factors, and all have good environmental adaptability because they still maintain relatively considerable recognition performance in a receiving environment that does not appear in the training data set. However, it can be observed that the decline of the recognition accuracy of the CNN model is more obvious. At the same time, CNN and CNN-LSTM models are sensitive to a mixture of three electromagnetic factors. The recognition accuracy of these two models drops below 65% under highly non-ideal conditions. However, the recurrence plot-Darknet53 classifier has achieved ideal results both in single non-ideal situations and in hybrid non-ideal situations, and the recognition rate is consistently above 0.9. This can be attributed to the stable expression of PRI sequences in various data receiving environments by recurrence plot. Compared with the CNN classifier, the CNN-LSTM classifier achievesbetterrecognitionresults,whichshowsthatthetiming information of the PRI sequence can provide effective recognition basis. The CNN classifier can only extract the structural features of the sequence, and when the receiving environment deteriorates, the ontology structure of different PRI modulations becomes difficult to distinguish, and that leads to the failure of the CNN classifier to achieve better recognition results.

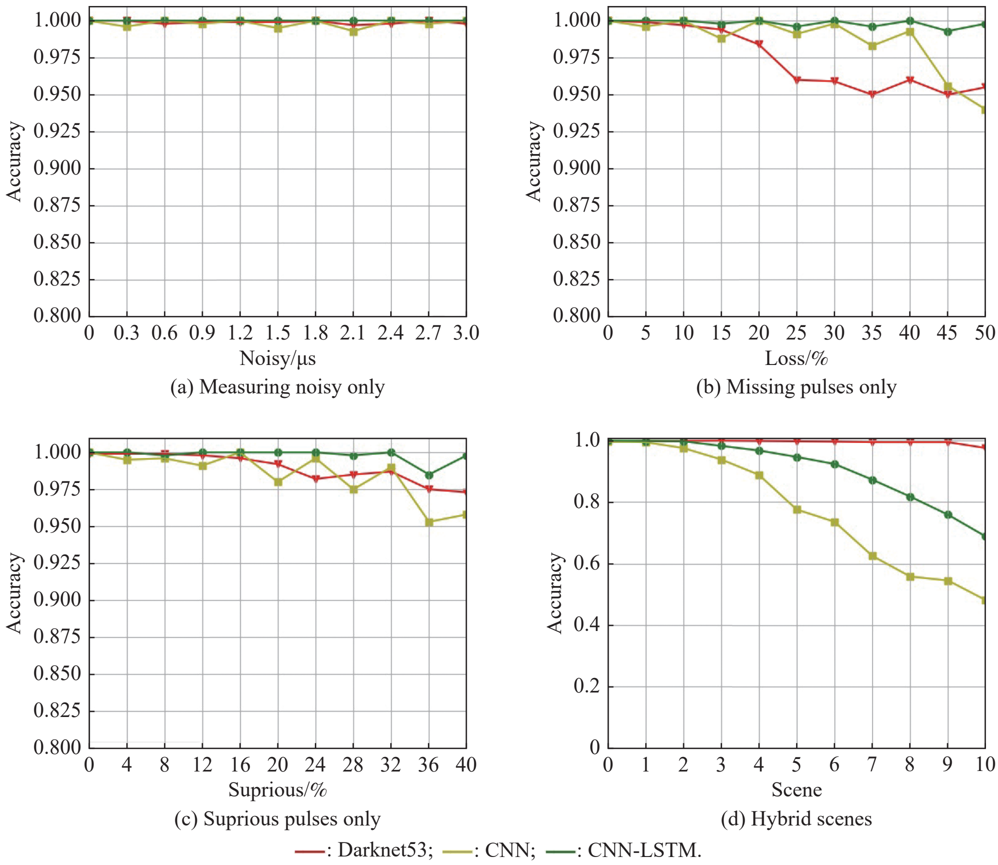

Fig. 7 Recognition accuracy in four non-ideal situations

In summary, although the PRI sequence can be directly sent to the network to achieve considerable recognition results, its performance is poor compared with the model using recurrence plot when running into highly non-ideal situations.

4.3 RP-YOLO framework

4.3.1 RP-YOLO implementation and identification results

The experiment in this section verifies the ability of the proposed RP-YOLO method to recognize dynamically varying RPI modulations. For the model to learn the characteristics of different modulations in a balanced way, each sequence in the training data set contains all six kinds of PRI modulations. The pulse length involved in each modulation is random, but not less than 100, and the total length of the sequence in the data set is 2000. While in the test sub-data, each sequence contains random types of modulation sequences (not less than one and not more than six), and the number of pulses involved in each modulation is also random. Also to verify the generalization ability of the model in different receiving situations, the training data set contains only six of eleven hybrid non-ideal scenes, namely scene 1, scene 3, scene 5, scene 7, scene 9 and scene 11, each with 1000 pieces of training data. The test data set includes 11 hybrid non-ideal scenes with 500 pieces of test data in each scene.

Fig. 8 shows four recognition results in four scenes, namely scene 1, scene 4, scene 9, and scene 11. Each subpicture is divided into two pictures. The ordinate of the upper picture represents the value of the PRI sequence, and the ordinate of the lower picture represents the classification result. In scene 1, where the sequence is ideal, the RP-YOLO method accurately identifies the categories of the six PRI modulations, and the transitions between different modulations are obvious, indicating that each modulation is precisely located. In the remaining three scenes, the sequences are damaged to different degrees, and the RP-YOLO method can still identify different categories of modulation, but the identified boundary is blurred. There are undetected fragments and partially incorrectly detected fragments in the head and tail of the subsequences. In scene 11, a highly non-ideal receiving environment causes an entire segment recognition error to occur. However, overall, the RP-YOLO method performs well in these four test sequences.

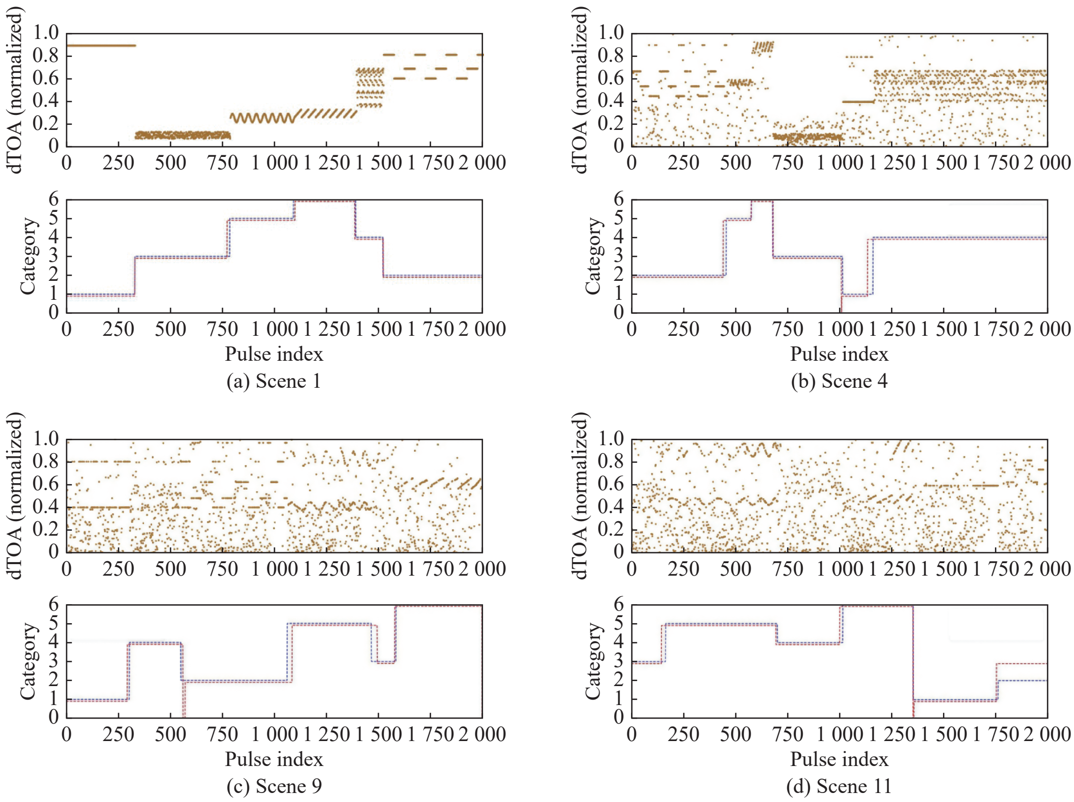

----: Ground_truth; ----: Predict.

Fig. 8 Detection results of the proposed method on PRI sequence with dynamic changes in modulation

4.3.2 Comparative experiment with other methods

A robust method should be able to identify correctly even the pulse sequencesare damaged. Denoted with a prefix sliding window (SL), CNN and CNN-LSTM models are added with appropriate sliding windows to form models that can continuously identify PRI modulation types on pulse sequence [4], and their performance is compared with the method proposed in this paper, which is represented as RP-YOLOv3 and RP-YOLOv4. Since the sliding window method is essentially a single-label classification model of PRI sequence, its performance is affected by the performance of CNN and CNN-LSTM models themselves: on the one hand, the input length of the two models should be consistent with the length of the sliding window; on the other hand, the longer the length of the input sequence, the more information the model can extract, and the more accurate the recognition will be. Therefore, the minimum length of each PRI modulation type in the PRI sequence will have a significant impact on the performance of the sliding window methods. This paper simulates two cases: one is that the number of pulses of each PRI modulation type is at least 200 and the corresponding sliding window width is set to 200; in another case, the number of pulses of each PRI modulation type is at least 400, and the corresponding sliding window length is set to 400.

The results are depicted in Fig. 9. As can be seen from the two figures, the performance of the sliding window method based on the CNN model has been greatly improved in the second case, and the recognition performance of the sliding window method based on the CNN-LSTM model has been slightly improved, while the recognition performance of RP-YOLO series methods remains basically unchanged. This shows that the longer the minimum length of each PRI modulation type is, the better the recognition performance of the sliding window method will be. When the length reaches a certain value, the recognition performance will tend to be stable. In addition, the recognition performance of the RP-YOLO series method is always better than that of the sliding window series method, and remains stable in two cases, indicating that it is not sensitive to the minimum length of each RPI modulation type in PRI sequences. The performance of the RP-YOLO method based on YOLOv4 is partially improved than that of YOLOv3, and the performance is more stable in different situations.

The experiment in this section runs on a desktop computer with an Intel Core i7-8700 3.20 GHz CPU and a Geforce RTX 2080 Ti GPU. The offline training time of the four networks is shown in Table 3, and the average time for each method to identify and process a sample with a length of 4 000 pulses is shown in Table 4. In terms of offline complexity, although the RP-YOLO method has a longer training time than CNN and CNN-LSTM models, its environment adaptability is stronger, and once the training is completed, it can be kept running without retraining. And the processing time of RP-YOLO series methods is within the acceptable range, so when facing the actual use environment, the method proposed in this article is practical. In summary, the RP-YOLO method is relatively balanced in training complexity and recognition performance.

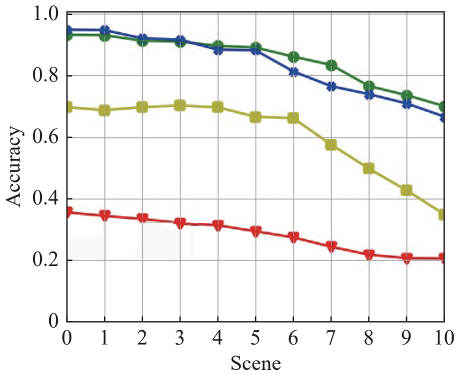

(a) Sliding window with 200 pulses

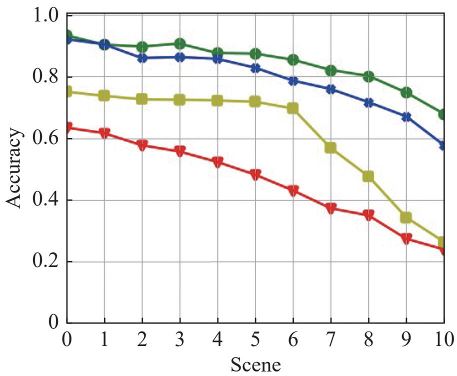

(b) Sliding window with 400 pulses

—: SL-CNN; —: SL-CNN-LSTM;
—: RP-YOLOv4; —: RP-YOLOv3.

Fig. 9 Recognition performance with different sliding window sizes

Table 3 Offline training time of different methods

Parameter	Method			
	SL-CNN	SL-LSTM	RP-YOLOv3	RP-YOLOv4
Training time /s	1 446	1 143	15 116	12 809
Training round	100	85	85	80

Table 4 Processing time of different methods

Parameter	Method			
	SL-CNN	SL-LSTM	RP-YOLOv3	RP-YOLOv4
Single sample processing time/s	0.08	0.95	0.18	0.13

4.3.3 Analysis of the influence of network parameters

In the target detection network based on priori anchor, the rationality of the priori anchor setting is very important to the performance of the final result. This article uses the K-means clustering algorithm to obtain nine sets of general priori anchors that are suitable for general scenes. Because all targets appear in the shape of a square in the recurrence plot, the width and height of the a priori anchor in this paper should be the same. In the end, this article calculates the parameters of the nine priori anchors as (10,10), (16,16), (23,23), (30,30), (62,62), (70,70), (116,116), (198,198) and (373,373). These anchors are assigned to three scale feature maps in the order of area from small to large. The feature map with a large scale uses the anchor frame with a small scale to calculate the coordinates and size information of the three prediction frames of each grid.

In this paper, 50 rounds of training are conducted using the above priori anchors and the priori anchors of coco dataset respectively. The curve of training loss is shown in Fig. 10. It can be seen that the priori anchors clustered by the K-means algorithm is more suitable for the data in this paper, and the priori anchors used in the coco dataset is mainly for the detection of general targets in nature, and its training loss converges to a larger value, which shows that the priori anchors obtained by the K-means algorithm is more effective.

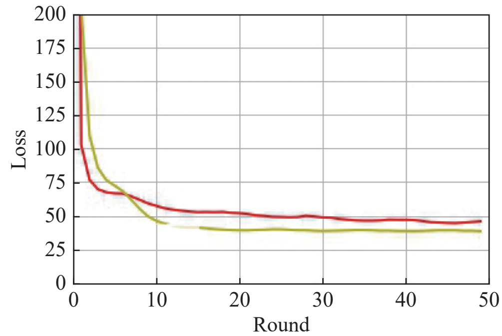

—: coco; —: K-means.

Fig. 10 Training loss curve of using different priori anchors

5. Conclusions

A new PRI modulation recognition method named RP-YOLO is proposed in this paper. In the RP-YOLO method, the recurrence plot is introduced into the representation of PRI sequences for the first time, and the problem of recognizing dynamically varying PRI modulations is creatively transformed into a multi-target detection problem. The RP-YOLO method can identify and locate various PRI modulations under highly non-ideal receiving conditions more effectively than the sliding window methods. Although this paper uses the recurrence plot technique to achieve the graphical representation of PRI sequences to adapt to the YOLO model, it is still meaningful to implement a variant of the YOLO model that can handle PRI sequences directly. The further work is to extract the modulation parameters of different modulations, which is of great significance for the quantitative analysis of radar working modes.

References

[1] NISHIGUCHI K, KOBAYASHI M. Improved algorithm for estimating pulse repetition intervals. IEEE Trans. on Aerospace and Electronic Systems, 2000, 36(2): 407–421.

[2] GENÇOL K, KARA A, AT N. Improvements on deinterleaving of radar pulses in dynamically varying signal environments. Digital Signal Processing, 2017, 69: 86–93.

[3] GENCOL K, AT N, KARA A. A wavelet-based feature set for recognizing pulse repetition interval modulation patterns. Turkish Journal of Electrical Engineering & Computer Sciences, 2016, 24(4): 3078–3090.

[4] KAUPPI J P, MARTIKAINEN K, RUOTSALAINEN U. Hierarchical classification of dynamically varying radar pulse repetition interval modulation patterns. Neural Networks, 2010, 23(10): 1226–1237.

[5] SHI R, WU C. Review on technology research about radar pulse signal deinterleaving based on PRI information. Telecommunication Engineering, 2020, 60(1): 112–120. (in Chinese)

[6] TORUN O, KOCAMIŞ M B, ABACI H, et al. Deinterleaving of radar signals with stagger PRI and dwell-switch PRI types. Proc. of the IEEE 25th Signal Processing and Communications Applications Conference, 2017: 1–4.

[7] HASANI H, KHOSRAVI M R. Pulse deinterleaving based on fusing PDWs and PRI extraction process for radar-assisted edge devices considering computational costs. EURASIP Journal on Wireless Communications and Networking, 2021(1): 1–14.

[8] GUAN Y F, ZHANG G Y. A radar emitter recognition method based on the PRI switching rules. Fire Control and Command Control, 2015, 40(3): 79–82. (in Chinese)

[9] LIU Z M. Recognition of multifunction radars via hierarchically mining and exploiting pulse group patterns. IEEE Trans. on Aerospace and Electronic Systems, 2020, 56(6): 4659–4672.

[10] RICHARD G, WILEY E. The interception and analysis of radar signals. Boston: Artech House, 2006.

[11] RAY P S. A novel pulse TOA analysis technique for radar identification. IEEE Trans. on Aerospace and Electronic Systems, 1998, 34(3): 716–721.

[12] WANG J P, CHU C Q. Approach to radar pulse repetition intervals modulation recognition based on Bayesian networks. Electronic Information Warfare Technology, 2007, 22(2): 14–17. (in Chinese)

[13] TAO R H, LI H S. A novel algorithm of radar signal recognition based on histogram and wavelet networks. Chinese Journal of Radio Science, 2005, 20(6): 784–788. (in Chinese)

[14] KAUPPI J P, MARTIKAINEN K S. An efficient set of features for pulse repetition interval modulation recognition. Proc. of the IET International Conference on Radar Systems, 2007: 1–5.

[15] MAHDAVI A, PEZESHK A M. A robust method for PRI modulation recognition. Proc. of the IEEE 10th International Conference on Signal Processing, 2010: 1873–1876.

[16] LIU Y C, ZHANG Q Y. An improved algorithm for PRI modulation recognition. Proc. of the IEEE International Conference on Signal Processing, Communications and Computing, 2017: 1–5.

[17] LI X Q, HUANG Z T, WANG F H, et al. Toward convolutional neural networks on pulse repetition interval modulation recognition. IEEE Communications Letters, 2018, 22(11): 2286–2289.

[18] NUHOĞLU M A. Classification of radar signal features in electronic warfare with convolutional long-short time memory. Proc. of the IEEE 26th Signal Processing and Communications Applications Conference, 2018: 1–4.

[19] ZHANG J Y, SU S Y. A method for the modulation pattern recognition of radar PRI based on fully convolutional neural network. Electronic Warfare Technology, 2020, 35(3): 40–45. (in Chinese)

[20] LI X, LIU Z, HUANG Z T. Attention-based radar PRI modulation recognition with recurrent neural networks. IEEE Access, 2020, 8: 57426–57436.

[21] WEI S Q, QU Q Z, WU Y T, et al. PRI modulation recognition based on squeeze-and-excitation networks. IEEE Communications Letters, 2020, 24(5): 1047–1051.

[22] ECKMANN J P, KAMPHORST S O, RUELLE D. Recurrence plots of dynamical systems. World Scientific Series on Nonlinear Science Series A, 1995, 16: 441–446.

[23] ZOLOTOVA N V, PONYAVIN D I. Phase asynchrony of the north-south sunspot activity. Astronomy & Astrophysics, 2006, 449(1): L1–L4.

[24] MARWAN N, TRAUTH M H, VUILLE M, et al. Comparing modern and Pleistocene ENSO-like influences in NW Argentina using nonlinear time series analysis methods. Climate Dynamics, 2003, 21(3/4): 317–326.

[25] NICHOLS J M, TRICKEY S T, SEAVER M. Damage detection using multivariate recurrence quantification analysis. Mechanical Systems and Signal Processing, 2006, 20(2): 421–437.

[26] REDMON J, DIVVALA S, GIRSHICK R, et al. You only look once: unified, real-time object detection. Proc. of the IEEE Conference on Computer Vision and Pattern Recognition, 2016: 779–788.

[27] REDMON J, FARHADI A. YOLO9000: better, faster, stronger. Proc. of the IEEE Conference on Computer Vision and Pattern Recognition, 2017: 7263-7271.

[28] REDMON J, FARHADI A. Yolov3: an incremental improvement. arXiv preprint arXiv: 1804.02767, 2018.

[29] BOCHKOVSKIY A, WANG C Y, LIAO H Y M. Yolov4: optimal speed and accuracy of object detection. arXiv preprint arXiv: 2004.10934, 2020.

[30] LI H, DENG L B, YANG C, et al. Enhanced YOLO v3 tiny network for real-time ship detection from visual image. IEEE Access, 2021, 9: 16692–16706.

[31] XU Q W, LIN R Z, YUE H, et al. Research on small target detection in driving scenarios based on improved yolo network. IEEE Access, 2020, 8: 27574–27583.

[32] CHEN H P, HE Z T, SHI B W, et al. Research on recognition method of electrical components based on YOLO V3. IEEE Access, 2019, 7: 157818–157829.

Biographies

WANG Pengcheng was born in 1998. He received his B.S. degree in the College of Communication Engineering from Jilin University in 2019. He is currently working toward his master's degree in the College of Communication Engineering from Jilin University, Jilin, China, in 2019. He is also working toward his master's degree in the State Key Laboratory of Complex Electromagnetic Environment Effects of Electronic Information System, National University of Defense Technology, Changsha. His current research interests include data mining and radar signal processing.
E-mail: wangpencheng19@163.com

LIU Weisong was born in 1993. He received his master's degree in information and communication engineering in 2015, from the College of Electronic Science and Engineering, National University of Defense Technology, Changsha, China. He is currently pursuing his Ph.D. degree in information and communication engineering with the State Key Laboratory of Complex Electromagnetic Environment Effects on Electronics and Information System, National University of Defense Technology. His research interests include radar and communication signal processing, and deep learning.
E-mail: liuweisong15@nudt.edu.cn

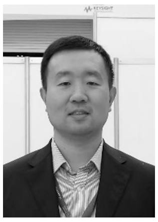

LIU Zheng was born in 1978. He is a researcher and Ph.D. supervisor of the State Key Laboratory of Complex Electromagnetic Environment Effects on Electronics and Information System, National University of Defense Technology. His research direction is intelligent electronic reconnaissance system and technology.
E-mail: liuzheng@nudt.edu.cn